Linkage and Solvent Dependence of Photoinduced Electron Transfer in Zincporphyrin-C_{60} Dyads

Hiroshi Imahori, Kiyoshi Hagiwara,[†] Masanori Aoki, Tsuyoshi Akiyama, Seiji Taniguchi,[†] Tadashi Okada,*[,†] Masahiro Shirakawa,[§] and Yoshiteru Sakata*

Contribution from the The Institute of Scientific and Industrial Research, Osaka University, Mihoga-oka, Ibaraki, Osaka 567, Japan

Received August 13, 1996[⊗]

Abstract: Four different kinds of C_{60}-linked zincporphyrins have been prepared by changing systematically the linking position at *meso*-phenyl ring from *ortho* to *para* and their photophysical properties have been investigated. Regardless of the linkage between the two chromophores, photoinduced charge separation (CS) and subsequent charge recombination (CR) were observed in a series of zincporphyrin-C_{60} dyads by picosecond fluorescence lifetime measurements and time-resolved transient absorption spectroscopy. In THF the CS occurs from both the excited singlet state of the porphyrin and the C_{60} moieties, implying that the increase of the absorption cross section by both the chromophores results in the efficient formation of the ion pair (IP) state. On the other hand, in benzene the IP state generated by the photoinduced CS from the excited singlet state of the porphyrin to the C_{60} produces or energetically equilibrates with the locally excited singlet state of the C_{60}. Both the CS and CR rates for the *meta* isomer are much slower than those for the other porphyrin-linked C_{60}. Linkage dependence of the electron transfer (ET) rates can be explained by superexchange mechanism via spacer. These results demonstrate that C_{60} is a new promising building block as an acceptor in artificial photosynthetic models.

Introduction

Photosynthesis is the elavorated natural system which converts light into useful chemical energy. The key reactions in photosynthesis are the photointiated energy transfer (EN) in the antenna complex and subsequent ET reaction in the reaction center. X-ray crystal analysis of the bacterial reaction center has revealed how well the constituted chromophores are arranged to achieve the IP state with a high quantum yield and a long lifetime.[1] There have been numerous attempts to mimic such supramolecular photoinitiated CS and ET relay in photosynthetic bacteria and plants. Especially, a number of donor (D)-spacer (S)-acceptor (A) molecules have been synthesized and the controlling factors in photosynthetic ET, such as separation distance, free energy changes, relative orientation, nature of the intervening medium, and temperature have been elucidated.[2] However, it is still difficult to construct artificial photoinduced CS and ET relay systems in terms of efficiency of CS as well as reaction mode because numbers of building blocks of D and/or A with high-performance are quite limited.[3]

Recently there appeared a new and attractive building block for an acceptor, i.e., fullerenes.[4] Especially C_{60} has the following characteristics;[5] (i) C_{60} consists of 60 carbon atoms and has large size (diameter, 8.8 Å, estimated from CPK model) as well as round shape. (ii) C_{60} has moderate electron-accepting abilities (−0.3 to −0.4 V vs SCE) similar to those of benzo- and naphthoquinones. (iii) Energy levels of the first excited singlet (2.00 eV) and triplet states (1.58 eV) of C_{60} are comparable to those of large π systems such as porphyrins and are much lower than those of small acceptors like quinones and pyromellitic diimides (>2 eV). (iv) C_{60} has rigid framework in the ground state and in the excited state and high stability under severe conditions. These characteristics are in sharp contrast with small-sized acceptors, such as benzoquinone and pyromellitic diimide, as well as large planar π acceptors, such as porphyrins and polycondensed aromatic compounds. There is a possibility that large and spherical acceptor like C_{60} shows peculiar ET dynamics different from those, shown in smaller counterparts and planar macrocycles. Although there are many reports on the participation of C_{60} in intermolecular ET processes,[6] less attention has been paid for intramolecular

[†] Department of Chemistry, Faculty of Engineering Science and Research Center for Extreme Materials, Osaka University, Toyonaka, Osaka 560, Japan.

[§] Nara Institute of Science and Technology, Ikoma, Nara 630-01, Japan.

[⊗] Abstract published in *Advance ACS Abstracts,* November 1, 1996.

(1) (a) Deisenhofer, J.; Epp, O.; Miki, K.; Huber, R.; Michel, H. *J. Biol. Chem.* **1984**, *180*, 385. (b) Chang, C.-H.; Tiede, D. M.; Tang, J.; Norris, J. R.; Schiffer, M. *FEBS Lett.* **1986**, *205*, 82. (c) Allen, J. P.; Feher, G.; Yeates, T. O.; Komiya, H.; Rees, D. C. *Proc. Natl. Acad. Sci. U.S.A.* **1987**, *84*, 5730.

(2) (a) Connolly, J. S.; Bolton, J. R. *In Photoinduced Electron Transfer, Part D*; Fox, M. A., Chanon, M., Eds.; Elsevier: Amsterdam, 1988; p 303. (b) Wasielewski, M. R. *In Photoinduced Electron Transfer, Part A*; Fox, M. A., Chanon, M., Eds.; Elsevier: Amsterdam, 1988; p 161. (c) Wasielewski, M. R. *Chem. Rev.* **1992**, *92*, 435. (d) Gust, D.; Moore, T. A.; Moore, A. L. *Acc. Chem. Res.* **1993**, *26*, 198. (e) Maruyama, K.; Osuka, A.; Mataga, N. *Pure Appl. Chem.* **1994**, *66*, 867. (f) Kurreck, H.; Huber, M. *Angew. Chem., Int. Ed. Engl.* **1995**, *34*, 849.

(3) (a) Nishitani, S.; Kurata, N.; Sakata, Y.; Misumi, S.; Karen, A.; Okada, T.; Mataga, N. *J. Am. Chem. Soc.* **1983**, *105*, 7771. (b) Gust, D.; Moore, T. A.; Moore, A. L.; Macpherson, A. N.; Lopez, A.; DeGraziano, J. M.; Gouni, I.; Bittersmann, E.; Seely, G. R.; Gao, F.; Nieman, R. A.; Ma, X. C.; Demanche, L. J.; Hung, S.-C.; Luttrull, D. K.; Lee, S.-J.; Kerrigan, P. K. *J. Am. Chem. Soc.* **1993**, *115*, 11141. (c) Wasielewski, M. R.; Niemczyk, M. P.; Svec, W. A.; Pewitt, E. B. *J. Am. Chem. Soc.* **1985**, *107*, 5562. (d) Sessler, J. L.; Capuano, V. L.; Harriman, A. *J. Am. Chem. Soc.* **1993**, *115*, 4618. (e) Ohkohchi, M.; Takahashi, A.; Mataga, N.; Okada, T.; Osuka, A.; Yamada, H.; Maruyama, K. *J. Am. Chem. Soc.* **1993**, *115*, 12137. (f) Harriman, A.; Odobel, F.; Sauvage, J.-P. *J. Am. Chem. Soc.* **1995**, *117*, 9461. (g) Osuka, A.; Marumo, S.; Mataga, N.; Taniguchi, S.; Okada, T.; Yamazaki, I.; Nishimura, Y.; Ohno, T.; Nozaki, K. *J. Am. Chem. Soc.* **1996**, *118*, 155. (h) Roest, M. R.; Verhoeven, J. W.; Schuddeboom, W.; Warman, J. M.; Lawson, J. M.; Paddon-Row, M. N. *J. Am. Chem. Soc.* **1996**, *118*, 1762.

(4) (a) Osawa, E. *Kagaku* (Chemistry) **1970**, *25*, 854. *Chem. Abstr.* **1971**, *74*(8): 75698v. (b) Kroto, H. W.; Heath, J. R.; O'Brien, S. C.; Curl, R. F.; Smalley, R. E. Nature **1985**, *318*, 162. (c) Krätschmer, W.; Lamb, L. D.; Fostiropoulos, K.; Huffman, D. R. *Nature* **1990**, *347*, 354.

(5) (a) Hirsch, A. *The Chemistry of the Fullerenes*; Georg Thieme Verlag: Stuttgart, 1994. (b) *Fullerenes*; Kadish, K. M., Ruoff, R. S., Eds.; The Electrochemical Society: NJ, 1995. (c) Foote, C. S. *Top. Curr. Chem.* **1994**, *169*, 347.

S0002-7863(96)02841-7 CCC: $12.00

systems involving C_{60}. Several groups have already reported the synthesis of D-linked fullerenes[7] including porphyrin-C_{60} linked systems,[7c,d,k−o] and some of them described the photoinduced intramolecular ET.[7c−f] However, systematic study for intramolecular photophysical processes of C_{60} is still lacking.

From the reasons described above, we designed and synthesized D-S-C_{60}. We chose porphyrin as a donor, since it is the most frequently employed building block in artificial photosynthetic models and therefore has the well-characterized photophysical properties. In the molecular design of porphyrin-C_{60} dyads, six *tert*-butyl groups were introduced into *meso*-phenyl rings of the porphyrin moiety to increase the solubility in usual organic solvents since porphyrins and fullerenes are notorious for their low solubility in these solvents.[8] C_{60} is covalently linked to a porphyrin aryl ring at three different positions, *para*, *meta*, and *ortho* via amido groups. In addition, cyclohexene ring fused to the C_{60} moiety is attached at 2,3-positions or 3,4-positions on the aromatic spacer when the *para* linkage is used. The spacer is relatively rigid so that it is possible to evaluate linkage and solvent dependence upon photophysical properties.

ET dynamics have been investigated by picosecond fluorescence lifetime measurements and picosecond time-resolved transient absorption spectroscopy. In this paper we describe only the zinc complex series because preliminary measurements indicate that the photophysical properties of the free base series are quite different from those of the zinc complex series.

Chart 1

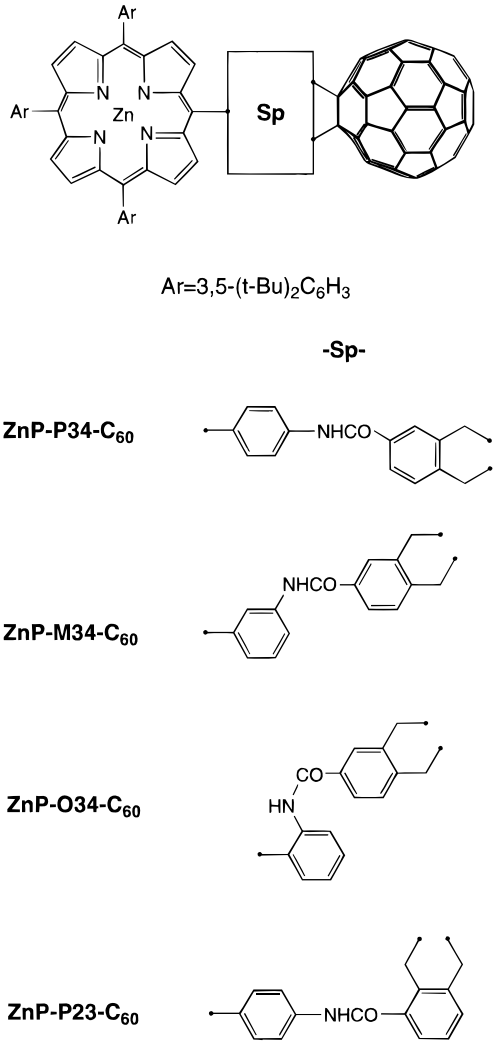

Investigations on the photophysics of the free base series are in progress and will be reported elsewhere.

Results

The synthesis and characterization of porphyrin-linked fullerenes and related model compounds are described in detail in the Supporting Information. The preliminary results have already been reported.[7d]

NMR Spectra. The porphyrin-linked fullerenes are expected to have relatively rigid geometry because of the double bond character of the amide bond in the spacer. However, there is still some freedom for rotation around single bonds in the linker. Detailed information on the geometry of the present compounds was given by ^{1}H NMR spectroscopy and molecular modeling.

ZnP-P34-C_{60}, **ZnP-P23-C_{60}**, **ZnP-M34-C_{60}**, and **ZnP-O34-C_{60}** exhibit a singlet set of ^{1}H NMR resonances at room temperature for each type of protons, indicating that they are either in a single conformation or in rapidly interexchanging conformations. The signals of the methylene protons of the cyclohexene ring in **ZnP-P34-C_{60}** appeared at 3.55 ppm as broad singlet, while in **ZnP-P23-C_{60}** appeared at 3.36, 3.42, and 4.43 ppm as broad singlet, in **ZnP-M34-C_{60}** appeared at 3.38, 3.56, and 3.64 ppm as broad singlet, and in **ZnP-O34-C_{60}** appeared at 2.18, 3.31, 3.62, and 3.74 ppm as doublet (Figure 1). These results show that the ring inversion of the cyclohexene ring becomes slower in the time scale of ^{1}H-NMR measurement in the order of the *para*, *meta*, and *ortho* linkages. It is interesting

(6) (a) Kamat, P. V. *J. Am. Chem. Soc.* **1991**, *113*, 9705. (b) Krusic, P. J.; Wasserman, E.; Parkinson, B. A.; Malone, B.; Holler, E. R., Jr.; Keizer, P. N.; Morton, J. R.; Preston, K. F. *J. Am. Chem. Soc.* **1991**, *113*, 6274. (c) Verhoeven, J. W.; Scherer, T.; Heymann, D. *Recl. Trav. Chim. Pays-Bas* **1991**, *110*, 349. (d) Sension, R. J.; Szarka, A. Z.; Smith, G. R.; Hochstrasser, R. M. *Chem. Phys. Lett.* **1991**, *185*, 179. (e) Arbogast, J. W.; Foote, C. S.; Kao, M. *J. Am. Chem. Soc.* **1992**, *114*, 2277. (f) Hwang, K. C.; Mauzerall, D. *J. Am. Chem. Soc.* **1992**, *114*, 9705. (g) Wang, Y. *J. Phys. Chem.* **1992**, *96*, 764. (h) Wang, Y. *Nature* **1992**, *356*, 585. (i) Williams, R. M.; Verhoeven, J. W. *Chem. Phys. Lett.* **1992**, *194*, 446. (j) Wang, Y.; West, R.; Yuan, C. H. *J. Am. Chem. Soc.* **1993**, *115*, 3844. (k) Dimitrijevic, N. M.; Kamat, P. V. *J. Phys. Chem.* **1993**, *97*, 7623. (l) Osaki, T.; Tai, Y.; Tazawa, M.; Tanemura, S.; Inukai, K.; Ishiguro, K.; Sawaki, Y.; Saito, Y.; Shinohara, H.; Nagashima, H. *Chem. Lett.* **1993**, 789. (m) Caspar, J. V.; Wang, Y. *Chem. Phys. Lett.* **1994**, *218*, 221. (n) Watanabe, A.; Ito, O. *J. Chem. Soc., Chem. Commun.* **1994**, 1285. (o) Guldi, D. M.; Neta, P.; Asmus, K.-D. *J. Phys. Chem.* **1994**, *98*, 4617. (p) Mikami, K.; Matsumoto, S.; Ishida, A.; Takamuku, S.; Suenobu, T.; Fukuzumi, S. *J. Am. Chem. Soc.* **1995**, *117*, 11134. (q) Ma, B.; Lawson, G. E.; Bunker, C. E.; Kitaygorodskiy, A.; Sun, Y. -P. *Chem. Phys. Lett.* **1995**, *247*, 51.

(7) (a) Khan, S. I.; Oliver, A. M.; Paddon-Row, M. N.; Rubin, Y. *J. Am. Chem. Soc.* **1993**, *115*, 4919. (b) Rasinkangas, M.; Pakkanen, T. T.; Pakkanen, T. A. *J. Organomet. Chem.* **1994**, *476*, C6. (c) Liddell, P. A.; Sumida, J. P.; Macpherson, A. N.; Noss, L.; Seely, G. R.; Clark, K. N.; Moore, A. L.; Moore, T. A.; Gust, D. *Photochem. Photobiol.* **1994**, *60*, 537. (d) Imahori, H.; Hagiwara, K.; Akiyama, T.; Taniguchi, S.; Okada, T.; Sakata, Y. *Chem. Lett.* **1995**, 265. (e) Imahori, H.; Cardoso, S.; Tatman, D.; Lin, S.; Noss, L.; Seely, G. R.; Sereno, L.; de Silber, J. C.; Moore, T. A.; Moore, A. L.; Gust, D. *Photochem. Photobiol.* **1995**, *62*, 1009. (f) Sariciftci, N. S.; Wudl, F.; Heeger, A. J.; Maggini, M.; Scorrano, G.; Prato, M.; Bourassa, J.; Ford, P. C. *Chem. Phys. Lett.* **1995**, *247*, 510. (g) Linssen, T. G.; Dürr, K.; Hanack, M.; Hirsch, A. *J. Chem. Soc., Chem. Commun.* **1995**, 103. (h) Diederich, F.; Dietrich-Buchecker, C.; Nierengarten, J.-F.; Sauvage, J.-P. *J. Chem. Soc., Chem. Commun.* **1995**, 781. (i) Maggini, M.; Dono, A.; Scorrano, G.; Prato, M.; *J. Chem. Soc., Chem. Commun.* **1995**, 845. (j) Williams, R. M.; Zwier, J. M.; Verhoeven, J. W. *J. Am. Chem. Soc.* **1995**, *117*, 4093. (k) Drovetskaya, T.; Reed, C. A.; Boyd, P. *Tetrahedron Lett.* **1995**, *36*, 7971. (l) Imahori, H.; Sakata, Y. *Chem. Lett.* **1996**, 199. (m) Ranasinghe, M. G.; Oliver, A. M.; Rothenfluh, D. F.; Salek, A.; Paddon-Row, M. N. *Tetrahedron Lett.* **1996**, *37*, 4797. (n) Schuster, D. I.; Cheng, P.; Wang, Y.; Wilson, S. R. *189th Annual Meeting of the Electrochemical Society*; Los Angeles, CA, May 1996; Abstract No. 680. (o) Akiyama, T.; Imahori, H.; Ajawakom, A.; Sakata, Y. *Chem. Lett.* **1996**, 907.

(8) (a) Miyamoto, T. K.; Tsuzuki, S.; Hasegawa, T.; Sasaki, Y. *Chem Lett.* **1983**, 1587. (b) Chardon-Noblat, S.; Sauvage, J.-P.; Mathis, P. *Angew. Chem., Int. Ed. Engl.* **1989**, *28*, 593. (c) Mammel, D.; Kautz, C.; Müllen, K. *Chem. Ber.* **1990**, *123*, 1353. (d) Tamiaki, H.; Suzuki, S.; Maruyama, K. *Bull. Chem. Soc. Jpn.* **1993**, *66*, 2633.

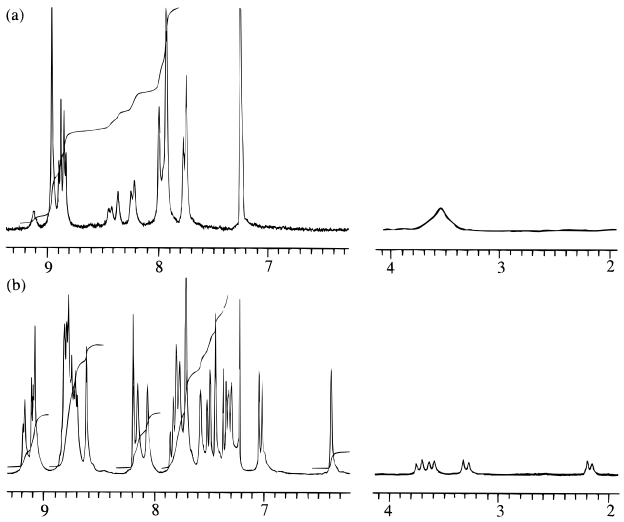

Figure 1. ^{1}H NMR spectra (270 MHz) of (a) **ZnP-P34-C_{60}** and (b) **ZnP-O34-C_{60}** in $CDCl_3$.

to note that in **ZnP-O34-C_{60}** unusual chemical shifts were observed. Thus, one of the methylene protons of the cyclohexene ring and one of the adjacent aromatic protons were shifted to upfield by 1−2 ppm, owing to the ring current effect of the porphyrin. Two of the β protons of pyrrole rings were shifted to downfield by about 0.5 ppm and five of the six *tert*-butyl groups are magnetically unequivalent, due to deshielding effect of the C_{60} ring.[9] This indicates that the C_{60} chromophore is closely located onto the porphyrin plane in **ZnP-O34-C_{60}**.

It has already been established on the basis of chemical shifts, X-ray analysis, and MO calculations that the Diels−Alder cycloaddition of *ortho*-quinodimethane with C_{60} occurs at the 6,6-ring junction of the C_{60} framework with closed transannular bond.[10] In ^{13}C NMR spectra of porphyrin-linked fullerenes, there exist one or two signals (63-65 ppm), which are quite close to the reported value (66−69 ppm) for the quarternary carbon at the 6,6-ring junction of the Diels−Alder adduct. This fact clearly shows that porphyrin-linked fullerenes have also the 6,6-closed structure.

Molecular Mechanics Calculations. Molecular mechanics calculations using the QUANTA/CHARMm program yielded the structures shown in Figure 2−5 as the lowest-energy conformation of porphyrin-linked fullerenes. An adopted basis Newton-Raphson method was used for energy minimization. The porphyrin and the C_{60} moieties are respectively minimized and are linked together. Three single bonds (ϕ_1,ϕ_2,ϕ_4) in the linker are rotated individually by 30 degrees. Each strucuture of 1728 different conformations generated are minimized constraining the structure of the porphyrin moiety to hold the planarity of the porphyrin ring observed by X-ray crystallography.[11] During all procedures the usual CHARMm parameters were retained to calculate the optimized structure for porphyrin-linked fullerenes.

Dihedral angles in the linker and center-to-center distances (edge-to-edge distances) are summarized in Table 1. **ZnP-P34-C_{60}** takes stretched conformation, while **ZnP-M34-C_{60}** and **ZnP-P23-C_{60}** adopt chair-like conformation with the closest separation distance between the two chromophores. The C_{60} moiety in **ZnP-O34-C_{60}** is folded onto the porphyrin ring. These results are consistent with the ^{1}H NMR spectra. As described later, the time scale for photochemical processes including ET is much faster compared with the usual rates of rotation about single bonds. Thus, these conformations can be used with confidence to discuss about the relationship between the structure and the ultrafast photodynamics.

Chart 2

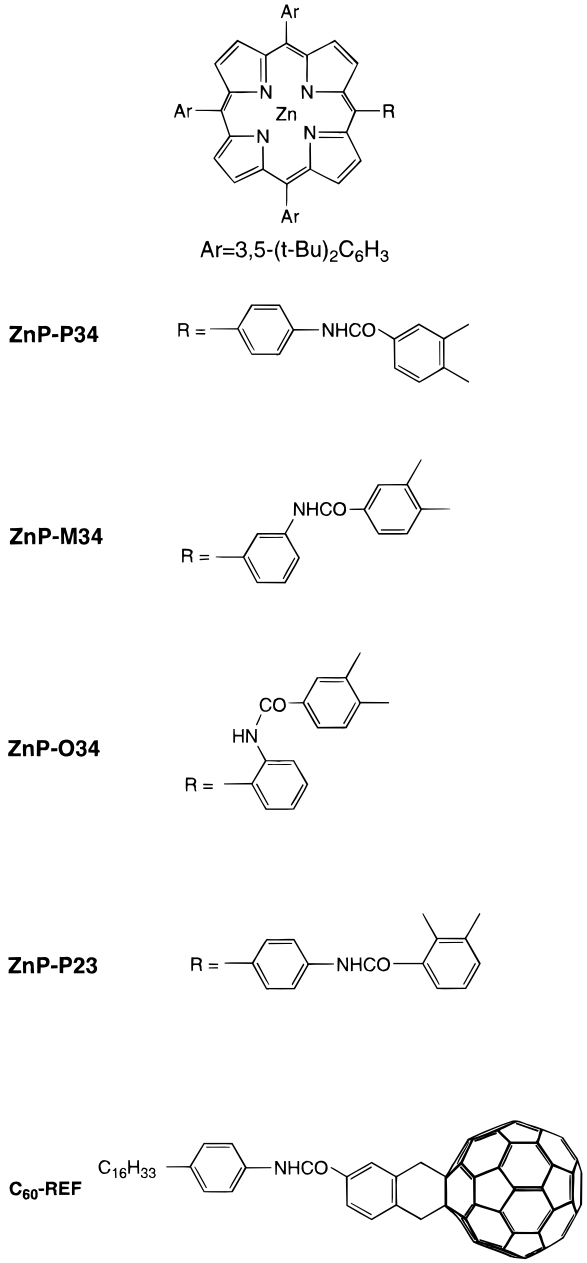

UV-vis Spectra. The spectra of **ZnP-P34-C_{60}**, **ZnP-M34-C_{60}**, and **ZnP-P23-C_{60}** in THF and benzene are essentially a linear combination of the absorption spectra of porphyrin references **ZnP-P34**, **ZnP-M34**, and **ZnP-P23** and C_{60} reference **C_{60}-REF**, respectively (Figure 6). There is no evidence for strong interactions between the two moieties. The absorption due to the C_{60} is much weaker and broader compared with the porphyrin. On the other hand, pronounced change was seen in the absorption spectra of **ZnP-O34-C_{60}** (Figure 7). The Soret band as well as Q-bands become quite broad and are shifted to longer wavelength by about 5−10 nm relative to **ZnP-O34**,

(9) Prato, M.; Suzuki, T.; Wudl, F.; Lucchini, V.; Maggini, M. *J. Am. Chem. Soc.* **1993**, *115*, 7876.

(10) (a) Belik, P.; Gügel, A.; Spickermann, J.; Müllen, K. *Angew. Chem., Int. Ed. Engl.* **1993**, *32*, 78. (b) Diederich, F.; Jonas, U.; Gramlich, V.; Herrmann, A.; Ringsdorf, H.; Thilgen, C. *Helv. Chim. Acta* **1993**, *76*, 2445. (c) Rubin, Y.; Khan, S.; Freedberg, D. I.; Yeretzian, C. *J. Am. Chem. Soc.* **1993**, *115*, 344. (d) Chikama, A.; Fueno, H.; Fujimoto, H. *J. Phys. Chem.* **1995**, *99*, 8541.

(11) Howard, J. L. *Porphyrins and Metalloporphyrins*; Smith, K. M., Ed.; Elsevier: New York, 1975; p 317.

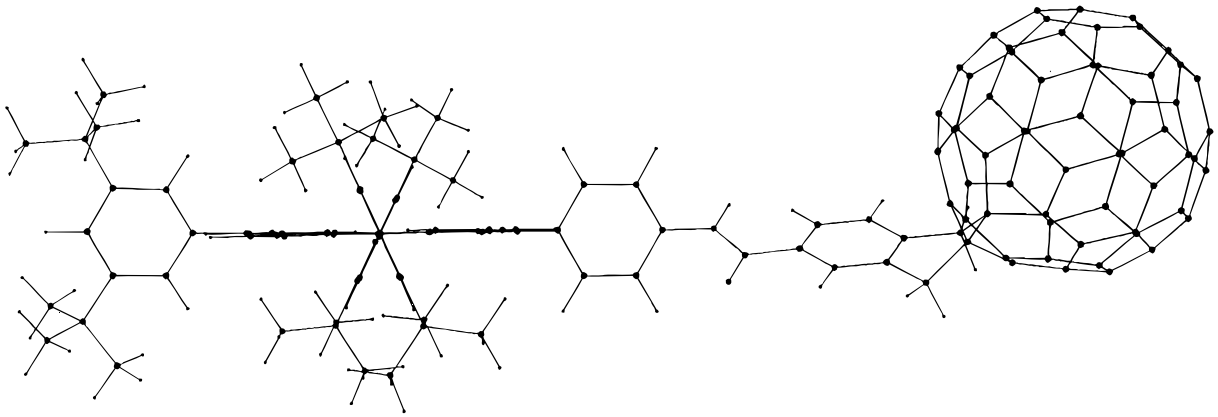

Figure 2. Lowest energy conformation of **ZnP-P34-C_{60}**.

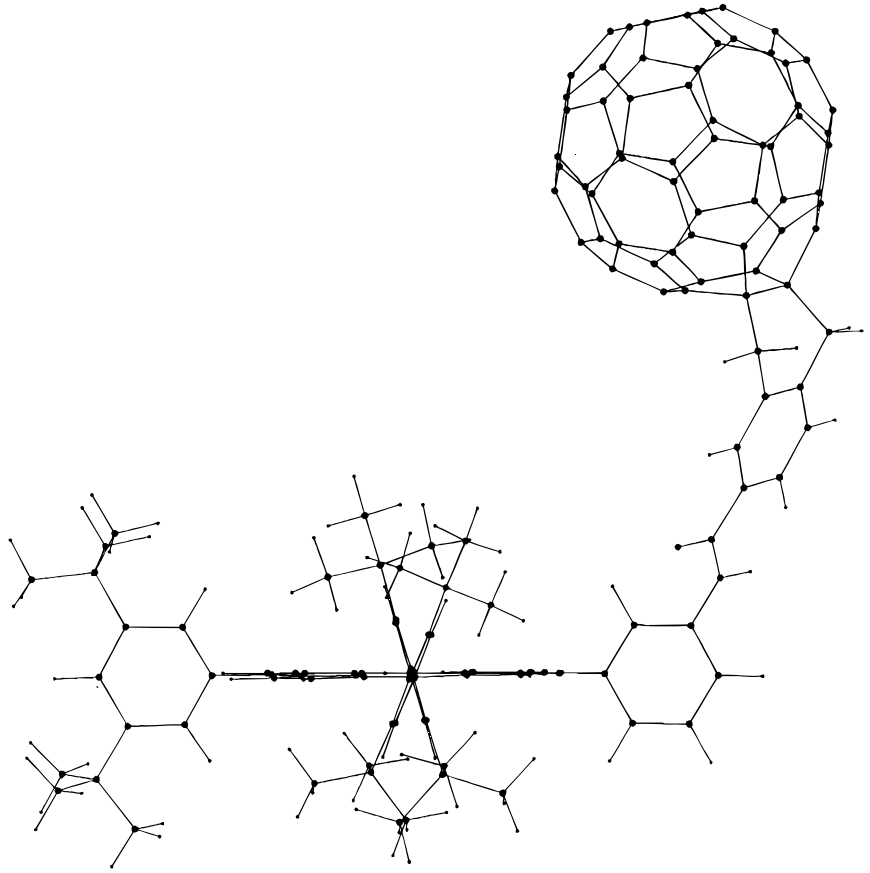

Figure 3. Lowest energy conformation of **ZnP-M34-C_{60}**.

indicating that there is considerable interaction between the two chromophores in the ground state.

Steady-State Fluorescence Spectra. Fluorescence spectra were taken in THF and benzene excited at 400 nm where both the porphyrin and the C_{60} absorb in a molar ratio of 4:1. Fluorescence spectra of **ZnP-P34-C_{60}**, **ZnP-M34-C_{60}**, **ZnP-O34-C_{60}**, and **ZnP-P23-C_{60}** in THF and benzene are strongly quenched compared with those of **ZnP-P34**, **ZnP-M34**, **ZnP-O34**, and **ZnP-P23**, respectively, showing the rapid quenching of the porphyrin excited singlet state by the attached C_{60}. **C_{60}-REF** shows weak emission with a peak maximum at 720 nm.[12] In THF emissions from both the porphyrin (580−680 nm) and the C_{60} (700−750 nm) moieties were observed in **ZnP-M34-C_{60}**, while no apparent C_{60} emission could be detected in **ZnP-P34-C_{60}**, **ZnP-O34-C_{60}**, and **ZnP-P23-C_{60}** (Figure 8). Very weak fluorescence from the C_{60} was detected when peak top of the Q-band in **ZnP-M34-C_{60}**, where almost solely the porphyrin absorbs, or at the same wavelength **C_{60}-REF** were excited in THF solutions of the same concentration. Therefore, we could not have clear evidence for the existence of the singlet−singlet EN from the porphyrin to the C_{60} in **ZnP-M34-C_{60}**. In benzene fluorescence from the C_{60} was clearly seen for all porphyrin-linked fullerenes in addition to the emission due to the porphyrin (Figure 8). Fluorescence from the C_{60} moiety was also observed clearly when peak top of the Q-band was excited in benzene where mainly the porphyrin absorbs. This indicates that in benzene there is a relaxation pathway from the excited singlet state of the porphyrin to that of the C_{60}.

(12) (a) Anderson, J. L.; An, Y.-Z.; Rubin, Y.; Foote, C. S. *J. Am. Chem. Soc.* **1994**, *116*, 9763. (b) Bensasson, R. V.; Bienvenue, E.; Janot, J.-M.; Leach, S.; Seta, P.; Schuster, D. I.; Wilson, S. R.; Zhao, H. *Chem. Phys. Lett.* **1995**, *245*, 566. (c) Nakamura, Y.; Minowa, T.; Tobita, S.; Shizuka, H.; Nishimura, J. *J. Chem. Soc., Perkin Trans. 2* **1995**, 2351.

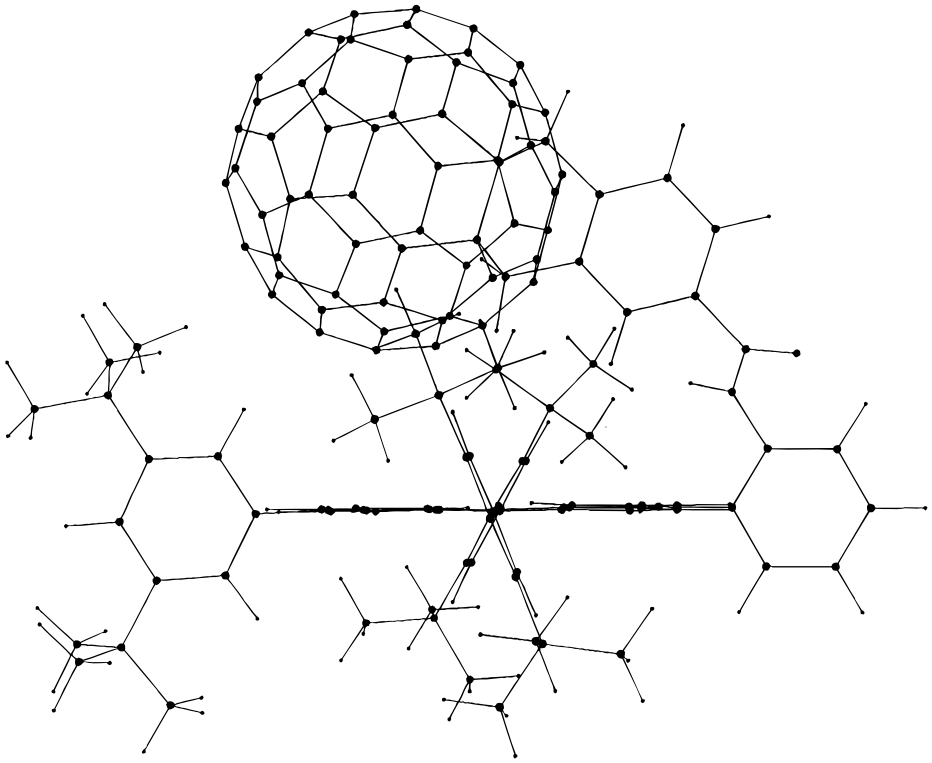

Figure 4. Lowest energy conformation of **ZnP-O34-C_{60}**.

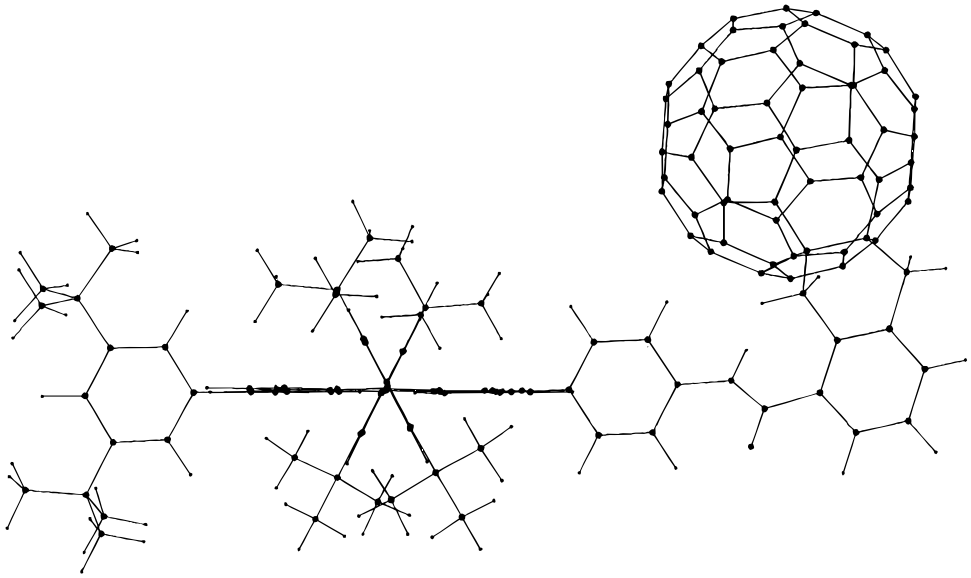

Figure 5. Lowest energy conformation of **ZnP-P23-C_{60}**.

Chart 3

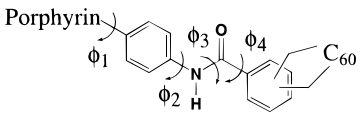

Fluorescence Lifetime Measurements. The fluorescence lifetimes of porphyrin-linked fullerenes were measured by a picosecond time-resolved single-photon counting technique. The dyad in THF or benzene was excited at 400−403 nm, where both the porphyrin and the C_{60} absorb in a molar ratio of 4:1. The fluorescence decay was monitored at 600-650, 720, and 750 nm, where the emission is due to only the porphyrin, both the porphyrin and the C_{60}, and mainly the C_{60}, respectively. The decay curves at 600−650 nm were fitted by one major exponential decays with 40−200 ps of lifetimes, indicating the existence of deactivation pathways from the excited singlet state of the porphyrin, such as ET and EN. On the other hand, the decay curves at 720 or 750 nm were fitted by the sum of two exponential decays. In each case, minor long-lived components were sensitive to the degree of purification of the samples, and, therefore, most probably are attributable to an impurity or decomposed samples. In a benzene solution of **ZnP-P34-C_{60}**

Table 1. Conformations of Porphyrin-Linked Fullerenes from Molecular Mechanics Calculations

compounds	ϕ_1	ϕ_2	ϕ_3	ϕ_4	R_{ee}[a]	R_{cc}[b]
ZnP-P34-C60	86.95	−48.64	179.07	−10.82	11.3	18.6
ZnP-M34-C60	95.86	51.17	−175.73	3.10	9.8	14.4
ZnP-O34-C60	−78.27	133.02	174.50	−129.15	3.2	7.6
ZnP-P23-C60	96.68	52.14	−175.81	−131.67	5.9	12.5

[a] Edge-to-edge distance in Å. [b] Center-to-center distance in Å.

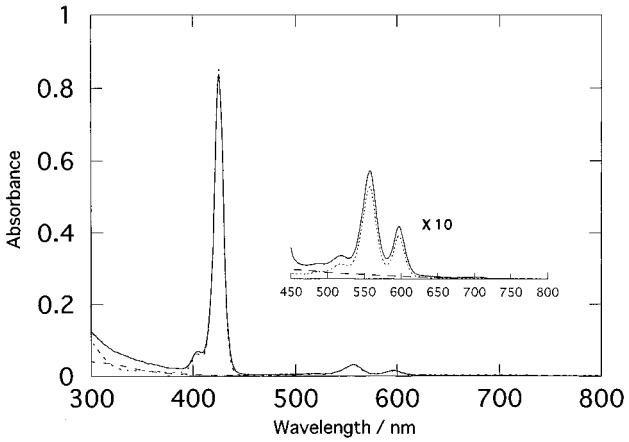

Figure 6. UV-visible absorption spectra of **ZnP-P34-C_{60}** (—), **ZnP-P34** (···), **C_{60}-REF** (- -) in THF (1.23×10^{-6} M).

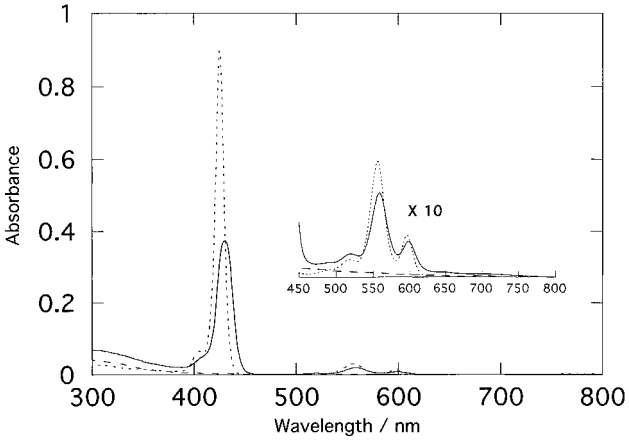

Figure 7. UV-visible absorption spectra of **ZnP-O34-C_{60}** (—), **ZnP-O34** (···), **C_{60}-REF** (- -) in THF (1.23×10^{-6} M).

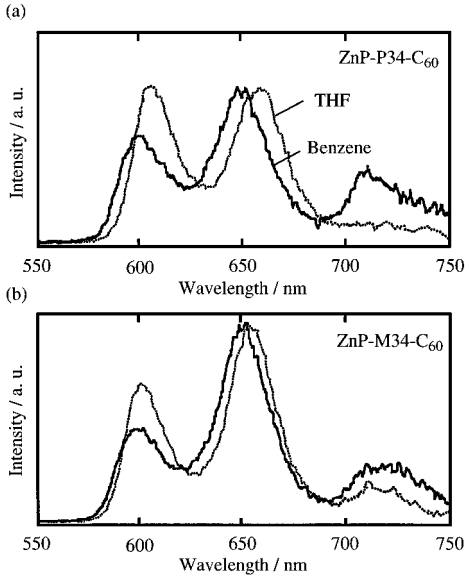

Figure 8. Fluorescence spectra of (a) **ZnP-P34-C_{60}** (THF, ···, benzene, —), and (b) **ZnP-M34-C_{60}** (THF, ···; benzene, —) excited at 400 nm. Spectra are corrected for the response of the detector system and normalized at the highest peak for the comparison.

and **ZnP-M34-C_{60}**, rise of the fluorescence with time constants of 490 and 830 ps, respectively, was seen clearly at 750 nm. The results are summarized in Table 2.

Time-Resolved Transient Absorption Spectroscopy. As an example of the time-resolved transient absorption spectra, results of **ZnP-P34-C_{60}** in THF are shown in Figure 9.

Scheme 1

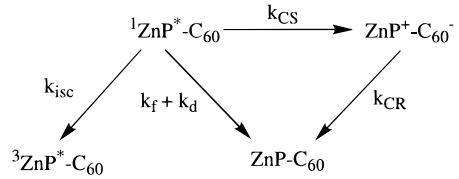

Immediately after excitation of **ZnP-P34-C_{60}** with 590 nm picosecond pulse, where both the porphyrin and the C_{60} were excited in a molar ratio of about 15:1, the bleaching of the ground state porphyrin absorption of the Q-bands at 560 and 600 nm and intense absorption with maximum at 470 nm were seen. With an increase of delay time, spectral change in an intense band with maximum at 460 nm appeared and broad bands with maxima around 650 and 900 nm arose and decayed simultaneously. We can tentatively assign the absorption bands around 650 and 900 nm to zincporphyrin cation radical (ZnP^+)[13] and C_{60} anion radical (C_{60}^-),[14] respectively.

The results in Figure 9 are depicted by Scheme 1, from which the time-dependent concentrations of the S_1[^{1}ZnP*-C_{60}], IP[ZnP^+-C_{60}^-], and T_1[^{3}ZnP*-C_{60}] states are given by the following equations:[15]

$$[S_1] = A_0 \exp(-t/\tau_{S1})$$

$$[IP] = \{A_0 \Phi_{CS} {\tau_{S1}}^{-1}/({\tau_{S1}}^{-1} - {\tau_{ion}}^{-1})\}\{\exp(-t/\tau_{ion}) - \exp(-t/\tau_{S1})\}$$

$$[T_1] = A_0(1 - \Phi_{CS})\Phi_T \{1 - \exp(-t/\tau_{S1})\}$$

where A_0 is the initial concentration of S_1, ${\tau_{S1}}^{-1} = k_{CS} + {\tau_{ref1}}^{-1}$, ${\tau_{ref1}}^{-1} = k_f + k_d + k_{isc}$, ${\tau_{ion}}^{-1} = k_{CR}$, $\Phi_{CS} = k_{CS}\tau_{S1}$, and $\Phi_T = k_{isc}\tau_{ref1}$. Since the decay of the T_1 state occurs in a much slower time scale compared with that of S_1 and ET, it is not necessary to take into account. The time profile of the transient absorbance $A_\lambda(t)$ at wavelength λ is obtained by the difference absorption coefficients of the S_1(ϵ_{S1}), the IP (ϵ_{ion}), and the T_1 (ϵ_{T1}) states at that wavelength as follows:

$$A_\lambda(t) = \epsilon_{S1}[S_1] + \epsilon_{ion}[IP] + \epsilon_{T1}[T_1] = A_1 \exp(-t/\tau_{S1}) + A_2 \exp(-t/\tau_{ion}) + A_3 \quad (1)$$

where $A_1 = A_0\{\epsilon_{S1} - \epsilon_{ion}\Phi_{CS}{\tau_{S1}}^{-1}/({\tau_{S1}}^{-1} - {\tau_{ion}}^{-1}) - \epsilon_{T1}(1 - \Phi_{CS})\Phi_T\}$, $A_2 = A_0\epsilon_{ion}\Phi_{CS}{\tau_{S1}}^{-1}/({\tau_{S1}}^{-1} - {\tau_{ion}}^{-1})$, and $A_3 = A_0\epsilon_{T1}(1 - \Phi_{CS})\Phi_T$.

By simulation of the observed time profiles at 470, 660, and 920 nm (Figure 10) with eq 1, values of τ_{S1} and τ_{ion} were obtained. Although both absorptions of C_{60} anion radical (C_{60}^-) and $S_n \leftarrow S_1$ of C_{60}[16] appear around 900−1000 nm, comcomitant rise (τ_{S1} = 100 ps) and decay (τ_{ion} = 500 ps) at 660-nm and 920-nm clearly show that the 650-nm band can be ascribed to ZnP^+ and the 900-nm band to C_{60}^-. In accordance with this

(13) (a) Fuhrhop, J. -H.; Mauzerall, D. J. *J. Am. Chem. Soc.* **1969**, *91*, 4174. (b) Chosrowjan, H.; Taniguchi, S.; Okada, T.; Takagi, S.; Arai, T.; Tokumaru, K. *Chem. Phys. Lett.* **1995**, *242*, 644.

(14) (a) Greaney, M. A.; Gorun, S. M. *J. Phys. Chem.* **1991**, *95*, 7142. (b) Dubois, D.; Kadish, K. M.; Flanagan, S.; Haufler, R. E.; Chibante, L. B. F.; Wilson, L. J. *J. Am. Chem. Soc.* **1991**, *113*, 4364. (c) Kato, T.; Kodama, T.; Shida, T.; Nakagawa, T.; Matsui, Y.; Suzuki, S.; Shiromaru, H.; Yamauchi, K.; Achiba, Y. *Chem. Phys. Lett.* **1991**, *180*, 446. (d) Gasyna, Z.; Andrews, L.; Schatz, P. *J. Phys. Chem.* **1992**, *96*, 1525.

(15) Asahi, T.; Ohkohchi, M.; Matsusaka, R; Mataga, N.; Zhang, R. P.; Osuka, A.; Maruyama, K. *J. Am. Chem. Soc.* **1993**, *115*, 5665.

(16) (a) Ebbesen, T. W.; Tanigaki, K.; Kuroshima, S. *Chem. Phys. Lett.* **1991**, *181*, 501. (b) Palit, D. K.; Sapre, A. V.; Mittal, J. P. *Chem. Phys. Lett.* **1992**, *195*, 1. (c) Bensasson, R. V.; Hill, T.; Lambert, C.; Land, E. J.; Leach, S.; Truscott, T. G. *Chem. Phys. Lett.* **1993**, *201*, 326.

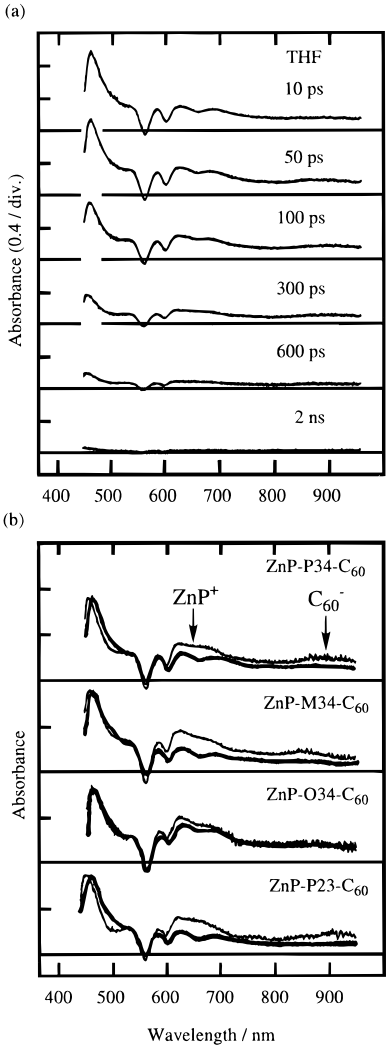

Figure 9. Time-resolved transient absorption spectra of (a) **ZnP-P34-C_{60}** and (b) **ZnP-P34-C_{60}**, **ZnP-M34-C_{60}**, **ZnP-O34-C_{60}**, and **ZnP-P23-C_{60}** at time delay of 20 ps (thick line) and 500 ps (thin line; 1 ns for **ZnP-M34-C_{60}**) excited at 590 nm in THF. Spectra in (b) are normalized at Soret bands for the comparison.

interpretation, the absorbance at 470 nm has biphasic decay with 100 and 500 ps, which are corresponding to the decay of ^{1}ZnP* and that of ZnP^+, respectively. Judging from the agreement of time constant for the decay of the fluorescence from the porphyrin (104 ps) and that for the rise time of the IP, the photoinduced CS and CR occur in **ZnP-P34-C_{60}**. From the rate constants $k_{CS} = 9.0 \times 10^9$ s^{-1} and $k_{ref1} = 1/\tau_{ref1} = 5.3 \times 10^8$ s^{-1}, yield of the IP, $k_{CS}/(k_{ref1} + k_{CS})$, is found to be almost unity, 0.94. Similarly, photoinduced CS and CR were observed in **ZnP-M34-C_{60}**, **ZnP-O34-C_{60}**, and **ZnP-P23-C_{60}** by picosecond time-resolved transient absorption spectroscopy (Figure 9). As for the cases in THF, similar spectral change with an increase of delay time in benzene was observed for **ZnP-P34-C_{60}**, **ZnP-M34-C_{60}**, **ZnP-O34-C_{60}**, and **ZnP-P23-C_{60}**, indicating formation of the IP state resulting from the photoinduced CS (Figure 11). One can clearly see the absorption band with maximum at 700 nm due to the triplet state localized in the C_{60} ($^3C_{60}$*),[16] in **ZnP-P23-C_{60}** at time delay of several nanosecond after the excitation. This assignment is supported by the fact that for **C_{60}-REF** the absorption with maximum at 700 nm rises at time delay of a few nanosecond with concomitant decay of the broad absorption around 700−1000 nm after the excitation. Both transient species are respectively corresponding to the excited triplet and singlet state of **C_{60}-REF**. In the cases for

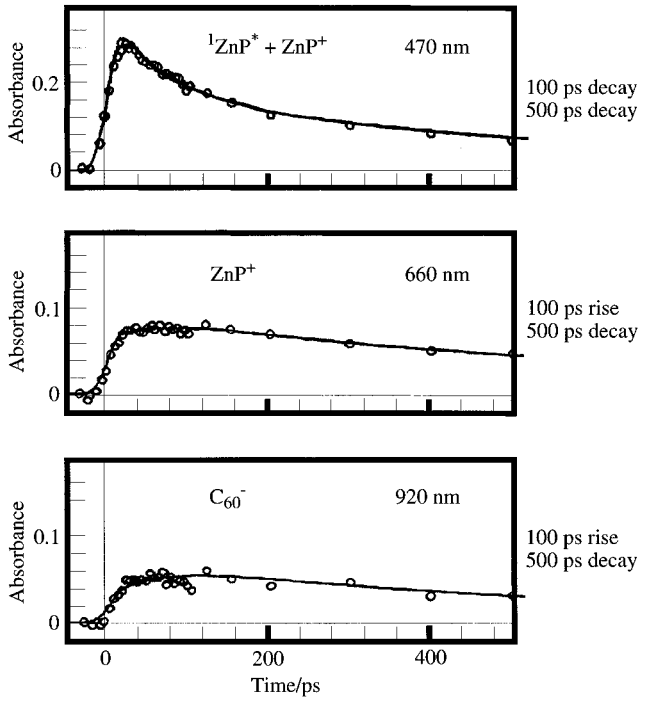

Figure 10. Time profiles in the transient absorption spectra of **ZnP-P34-C_{60}** at 470 nm (top), 660 nm (middle), and 920 nm (bottom) in THF.

ZnP-P34-C_{60}, **ZnP-M34-C_{60}**, and **ZnP-O34-C_{60}**, weak transient absorptions due to $^3C_{60}$* are seen at time delay of several nanosecond after the excitation, which is consistent with those of the steady-state fluorescence. These results also suggest that there exists a relaxation pathway from ^{1}ZnP* to $^1C_{60}$*. Values of τ_{S1} and τ_{ion} obtained by analyzing the absorbance changes of transient species are summarized in Table 2.

Estimation of Energy Level. Table 3 shows the energy levels of the locally excited singlet states of the porphyrin and the C_{60} and free energy changes. The energies of the 0−0 transition between the S_1 and the S_0 state were determined by averaging the energies of the corresponding (0, 0) peaks in the fluorescence and the absorption bands. Free energy changes, $-\Delta G_{CS}$ and $-\Delta G_{CR}$, were calculated by the Marcus and Born equation.[17,18] E_{ox} and E_{red} are the half-wave potentials of one-electron oxidation of the porphyrin and one-electron reduction of the C_{60}, respectively, in CH_2Cl_2 and they were obtained by differential pulse voltammetry (see the Supporting Information). Redox potentials of **ZnP-P34-C_{60}**, **ZnP-M34-C_{60}**, **ZnP-O34-C_{60}**, and **ZnP-P23-C_{60}** in CH_2Cl_2 using 0.1 M Bu_4NClO_4 as a supporting electrolyte are roughly explained by the sums of **ZnP-P34**, **ZnP-M34**, **ZnP-O34**, and **ZnP-P23** and **C_{60}-REF**, respectively. ΔG_s is the correction term for the effects of solvent polarity as well as the Coulombic energy between D^+ and A^-. In benzene solution the Born equation does not give correct values for ΔG_s because it overestimates the polarity of benzene. Therefore, we have used tentatively the value for $\Delta G_s = 0.4$ eV in benzene solution assuming that the value of ΔG_s for porphyrin-linked fullerenes is identical to that of porphyrin-linked quinones reported previously.[15]

Discussion

As mentioned above, the kinetic and spectroscopic data for porphyrin-linked fullerenes support the photoinduced CS and

(17) (a) Marcus, R. A. *J. Chem. Phys.* **1956**, *24*, 966. (b) Marcus, R. A. *J. Chem. Phys.* **1957**, *26*, 867. (c) Marcus, R. A.; Sutin, N. *Biochim. Biophys. Acta* **1985**, *811*, 265.

(18) Weller, A. Z. *Phys. Chem. (Wiesbaden)* **1982**, *93*, 1982.

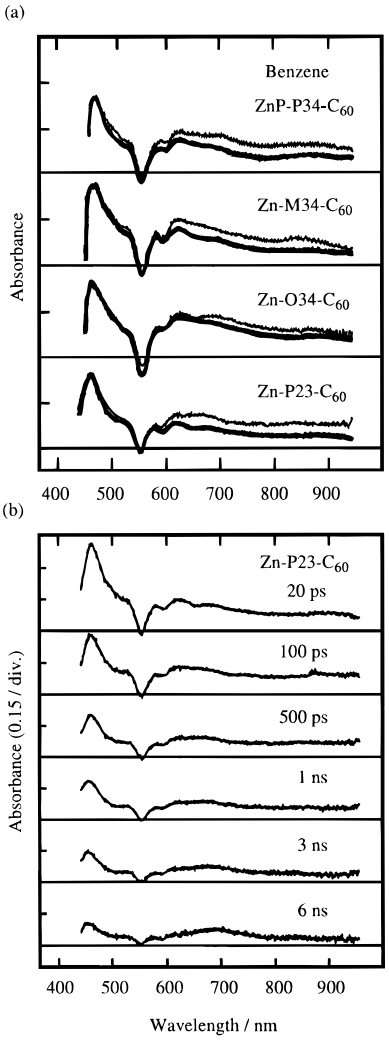

Figure 11. Time-resolved transient absorption spectra of (a) **ZnP-P34-C_{60}**, **ZnP-M34-C_{60}**, **ZnP-O34-C_{60}**, and **ZnP-P23-C_{60}** at time delay of 20 ps (thick line) and 500 ps (thin line) excited at 590 nm in benzene and (b) **ZnP-P23-C_{60}** in benzene. Spectra in (a) are normalized at Soret bands for the comparison.

CR. Comparison of the results for these molecules can help us elucidate the controlling factors in the photoinduced CS and CR in porphyrin-C_{60} systems. The best way to discuss the results is to investigate systematic variation in solvent and linkage for these molecules and compare the performance of them with other typical acceptors.

Reaction Scheme in Benzene. The lifetimes of the first excited singlet state of the porphyrin obtained by picosecond time-resolved transient absorption spectroscopy agree well with those obtained by fluorescence lifetime measurements as shown in Table 2. Therefore, the CS occurs immediately after the excitation of the porphyrin, ruling out the possibility of fast EN from the porphyrin to the C_{60}. In benzene dynamic behavior is quite different from that in THF as mentioned later. Thus, in addition to fluorescence from the porphyrin, a new fluorescence band due to the C_{60} is clearly seen in the region of 680−800 nm by the steady-state fluorescence measurements as shown in Figure 8. In addition, the time constants for rise components of the fluorescence at 750 nm, due to the C_{60}, in **ZnP-P34-C_{60}** and **ZnP-M34-C_{60}** and for the decay of the IP obtained by picosecond time-resolved transient absorption spectroscopy are almost the same in benzene, implying that the CR leads to the formation of $^1C_{60}$*, which shows delayed fluorescence.[19] On the other hand, there is no agreement between time constants of the decay of the porphyrin excited singlet state and rise of the fluorescence from the C_{60}. These results definitely eliminate the possibility of direct singlet−singlet EN from the porphyrin to the C_{60}. Time constant for the decay of the fluorescence from the C_{60} after the rise is about 1.4−1.5 ns, which is close to that of **C_{60}-REF**, suggesting that there is no additional relaxation pathway from $^1C_{60}$*, such as ET and EN. These results are quite consistent with the fact that $^3C_{60}$* was seen in benzene at time delay of nanosecond after the excitation. Therefore, we can conclude that energy level of the IP state in benzene is located between ^{1}ZnP* (2.08 eV) and $^1C_{60}$* (1.73 eV) for **ZnP-P34-C_{60}** and **ZnP-M34-C_{60}** as shown in Figure 12.

On the other hand, **ZnP-P23-C_{60}** is different from **ZnP-P34-C_{60}** and **ZnP-M34-C_{60}** in the points that no rise and dual exponential decay of the fluorescence at 750 nm were observed. Both the time constants (590 ps and 2900 ps) at 750 nm are not consistent with that (57 ps) due to the porphyrin at 650 nm, showing that the time constants at 750 nm are attributed to the C_{60}. Considering that time constant of the second component (2900 ps) agrees well with that of the IP (3000 ps), ZnP-$^1C_{60}$* and ZnP^+-C_{60}^- are energetically in equilibrium.[15,20] Thus, the time constants (590 and 2900 ps) are due to the decay of $^1C_{60}$* and to that of the IP, respectively. These results are consistent with the fact that in **ZnP-P23-C_{60}** $^3C_{60}$* is clearly seen by the transient absorption spectroscopy. It can be rationalized by the energy level diagram that energy level of the IP in **ZnP-P23-C_{60}** is comparable to that of $^1C_{60}$* (1.73 eV). Accordingly, we can experimentally estimate the value of the correction term, ΔG_s, is 0.29 eV for **ZnP-P23-C_{60}** in benzene (Figure 13).

Reaction Scheme in THF. As in benzene, lifetimes of the first excited singlet state of the porphyrin obtained by picosecond time-resolved transient absorption spectroscopy are good agreement with those obtained by fluorescence lifetime measurements. These results show obviously that the CS occurs immediately after the excitation of the porphyrin. No apparent fluorescence from the C_{60} was detected except for **ZnP-M34-C_{60}** by the steady-state fluorescence spectroscopy. However, very weak fluorescence due to the C_{60} was observed by the fluorescence lifetime measurements where lifetime of the fluorescence (400−800 ps) is shorter relative to that of **C_{60}-REF** (1.4 ns). Based on the energy level diagram it seems that CS also occurs from $^1C_{60}$* to the porphyrin. In steady-state fluorescence measurement apparent fluorescence due to the C_{60} is seen for **ZnP-M34-C_{60}**. Lifetime of the fluorescence from the C_{60} (1.2 ns) is quite similar to that of **C_{60}-REF**, implying that the excited singlet state of the C_{60} is not strongly quenched by the porphyrin in **ZnP-M34-C_{60}** compared to the other cases in THF. These results also support relaxation pathways from the excited singlet states of the two chromophores as shown in Figure 14.[21]

There is an another competitive pathway, where EN from ^{1}ZnP* takes place to populate the $^1C_{60}$*, followed by ET from the porphyrin to the $^1C_{60}$* to produce the IP state. The same match of the porphyrin fluorescence lifetime with the rise of the IP might be observed if the rate limiting step was EN.

(19) (a) Weller, A.; Zachariasse, K. *Chem. Phys. Lett.* **1971**, *10*, 424. (b) Weller, A.; Zachariasse, K. *Chem. Phys. Lett.* **1971**, *10*, 590.

(20) (a) Gain, G. L.; O'Neil, M. P.; Svec, W. A.; Niemczyk, M. P.; Wasielewski, M. R. *J. Am. Chem. Soc.* **1991**, *113*, 719. (b) Heitele, H.; Finck, S.; Weeren, S.; Pollinger, F.; Michel-Beyerle, M. *J. Phys. Chem.* **1989**, *93*, 5173.

(21) There is a discrepancy for time constants of the porphyrin fluorescence at 600−650 nm and 720 nm in some cases. Since k_{CS} and k_{CR} were obtained by simulating time profiles of the absorbances due to the transient species on the basis of the time constants of the porphyrin fluorescence, such mismatching may be caused by the experimental difficulty of determining fluorescence lifetime accurately using our instrumentation when the lifetime is less than 60 ps.

Table 2. Fluorescence Lifetimes of Dyads[a] and Lifetimes of ^{1}ZnP*-C_{60} (τ_{S1}) and ZnP^+-C_{60}^- (τ_{ion}) States

		fluorescence lifetime measurements			transient absorption spectroscopy	
compounds	solvents	λ_{obs} (nm)	τ_1[b] (ps)	τ_2[b] (ps)	τ_{S1} (ps)	τ_{ion} (ps)
ZnP-P34-C_{60}	benzene	600	81 (0.99)		80	500
ZnP-P34-C_{60}	benzene	750	rise 490 (−0.46)	1400 (1)		
ZnP-P34-C_{60}	THF	610	104 (0.88)		100	500
ZnP-P34-C_{60}	THF	720	92 (0.86)	780 (0.14)		
ZnP-M34-C_{60}	benzene	650	200 (0.97)		200	800
ZnP-M34-C_{60}	benzene	750	rise 830 (−0.59)	1500 (1)		
ZnP-M34-C_{60}	THF	650	200 (0.98)		200	4500
ZnP-M34-C_{60}	THF	750	200 (0.57)	1200 (0.43)		
ZnP-O34-C_{60}	benzene	610	93 (0.99)		90	350
ZnP-O34-C_{60}	benzene	750	230 (0.76)	1200 (0.24)		
ZnP-O34-C_{60}	THF	610	48 (0.97)		50	300
ZnP-O34-C_{60}	THF	720	80 (0.82)	390 (0.18)		
ZnP-P23-C_{60}	benzene	650	57 (0.99)		60	3000
ZnP-P23-C_{60}	benzene	750	590 (0.60)	2900 (0.40)		
ZnP-P23-C_{60}	THF	650	45 (0.99)		40	700
ZnP-P23-C_{60}	THF	720	74 (0.77)	400 (0.23)		

[a] Fluorescence lifetimes of **ZnP-P34**, **ZnP-M34**, **ZnP-O34**, and **ZnP-P23** in THF and benzene were 1.9−2.0 ns (= τ_{ref1}), while that of **C60-REF** was 1.4 ns (= τ_{ref2}) in the both solvents. [b] Numbers in parentheses are relative amplitudes of pre-exponential factors in exponential functions.

Table 3. Free Energy Changes and ET Rate Constants in Benzene and THF

compounds	solvents	ΔE^1_{0-0}[a] (eV)	ΔE^2_{0-0}[a] (eV)	$-\Delta G_{CS1}$[b] (eV)	$-\Delta G_{CS2}$[b] (eV)	$-\Delta G_{CR}$[b] (eV)	k_{CS1}[c] (10^9 s^{-1})	k_{CS2}[c] (10^9 s^{-1})	k_{CR}[c] (10^9 s^{-1})
ZnP-P34-C_{60}	benzene	2.08	1.73	0.26	−0.09	1.82	12		<2.0
ZnP-P34-C_{60}	THF	2.06	1.73	0.67	0.34	1.39	9.0	0.57	2.0
ZnP-M34-C_{60}	benzene	2.08	1.73	0.31	−0.04	1.77	4.5		<1.3
ZnP-M34-C_{60}	THF	2.06	1.73	0.75	0.42	1.31	4.5	0.12	0.22
ZnP-O34-C_{60}	benzene	2.08	1.73	0.22	−0.13	1.86	10		2.9
ZnP-O34-C_{60}	THF	2.06	1.73	0.79	0.46	1.27	20	1.9	3.3
ZnP-P23-C_{60}	benzene	2.08	1.73	0.24	−0.11	1.84	17		0.33
ZnP-P23-C_{60}	THF	2.06	1.73	0.70	0.37	1.36	22	1.8	1.4

[a] ΔE^1_{0-0} and ΔE^2_{0-0} are energies of the 0−0 transition between the S_1 and S_0 state for the porphyrin and the C_{60}, respectively. [b] $-\Delta G_{CR} = E_{ox} - E_{red} + \Delta G_s$, $-\Delta G_{CS} = \Delta E_{0-0} - (-\Delta G_{CR})$, $\Delta G_s = e^2/(4\pi\epsilon_0)[(1/(2R^+) + 1/(2R^-) - 1/R_{cc})(1/\epsilon_s) - (1/(2R^+) + 1/(2R^-))(1/\epsilon_r)]$ where E_{ox} and E_{red} are the first oxidation potential of the porphyrin and the first reduction potential of the C_{60} in CH_2Cl_2, respectively, R^+ and R^- are radii of D and A, respectively, and ϵ_s and ϵ_r are static dielectric constants of solvent used and when measured the redox potentials, respectively. R^+ and R^- were determined from CPK molecular modeling using CAChe. $R^+ = 5.0$ Å for the porphyrin, $R^- = 4.4$ Å for the C_{60}, $\epsilon_s = 7.4$ in THF, and $\epsilon_r = 8.9$ in CH_2Cl_2 are used for the calculations. In benzene, $\Delta G_s = 0.40$ eV is used. CS1 and CS2 are corresponding to CS from the excited singlet state of the porphyrin to the C_{60} and from that of the C_{60} to the porphyrin, respectively. [c] $k_{CS1} = \tau_1^{-1}$ (at 600−650 nm) $- \tau_{ref1}^{-1}$, $k_{CS2} = \tau_2^{-1}$ (at 720 or 750 nm) $- \tau_{ref2}^{-1}$, and $k_{CR} = \tau_{ion}^{-1}$.

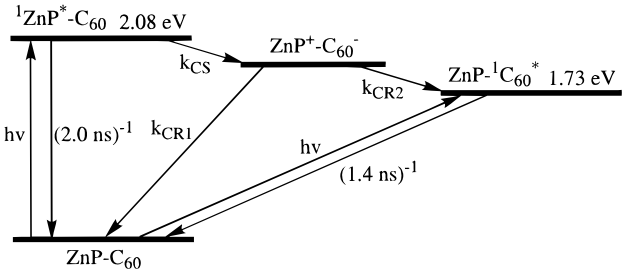

Figure 12. Schematic energy levels and relaxation pathways for the porphyrin and the C_{60} first excited states of **ZnP-P34-C_{60}** and **ZnP-M34-C_{60}** in benzene.

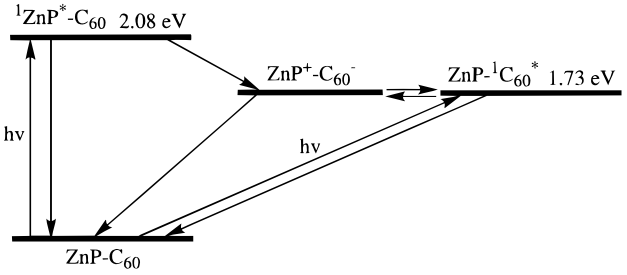

Figure 13. Schematic energy levels and relaxation pathways for the porphyrin and the C_{60} first excited states of **ZnP-P23-C_{60}** in benzene.

However, the fact that faster ET rates ($4.5-22 \times 10^9$ s^{-1}) from the ^{1}ZnP* to the C_{60}, compared with those ($0.12-1.9 \times 10^9$ s^{-1}) from the $^1C_{60}$* to the porphyrin are observed, rules out the initial EN and subsequent ET pathway. Direct ET pathway is also supported by the fact that (1) in benzene stepwise formation of $^1C_{60}$* the initial CS and subsequent energy migration was observed with a time constant of 500−800 ps as it has been already discussed, (2) in THF no fluorescence from the C_{60} was detected when the Q-band was excited where mainly the porphyrin absorbs, and (3) there is no large overlap of fluorescence from the porphyrin and absorption of the C_{60}, remarkably reducing the probability of the EN.[22] We can also rule out the possibility that there is fast energy equilibrium between ^{1}ZnP* and $^1C_{60}$* because of relatively large energy gap (>0.3 eV) between the two states.[15,20]

Ortho Isomer. As one can see from ^{1}H NMR spectra, molecular modeling, and UV-vis absorption spectra of **ZnP-O34-C_{60}**, there is significant interaction between the porphyrin and C_{60} moieties. The time-resolved transient absorption immediately after the excitation is similar to those of the IP state in other porphyrin-linked C_{60}. Spectral change due to the transient species is smaller with an increase of delay time

(22) Turro, N. J. *Modern Molecular Photochemistry*; The Benjamin & Cummings: Menlo Park, 1978; p 296.

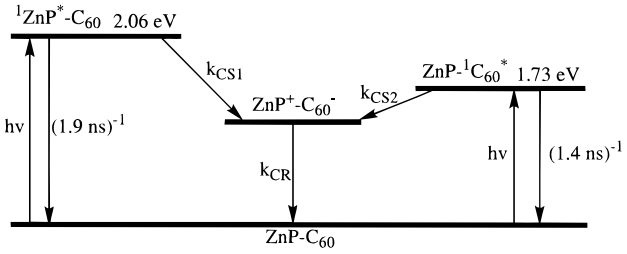

Figure 14. Schematic energy levels and relaxation pathways for the porphyrin and the C_{60} first excited states of **ZnP-P34-C$_{60}$**, **ZnP-M34-C$_{60}$**, and **ZnP-P23-C$_{60}$** in THF.

compared with other porphyrin-linked C_{60}. In addition, two components of fluorescence decay at 750 nm were observed in benzene. The time constants were not consistent with those due to the porphyrin or to the IP, suggesting that the two decay components at 750 nm are derived from the $^1C_{60}$*. In both benzene and THF the time constants of the fluorescence decay from the porphyrin agree well with those of rise due to the formation of the IP. Although it seems that the main pathway is photoinduced CS and CR, other pathways like formation of the exciplex or due to the conformational difference might occur.[23]

Gust and Moore *et al.* reported porphyrin-C_{60} dyads in which the two chromophores are linked by a bicyclic bridge.[7c] The zinc dyad exhibits rapid and efficient singlet−singlet EN (2×10^{11} s^{-1}) from the porphyrin to the C_{60} followed by ET (2×10^{11} s^{-1}) to yield the IP state in both benzonitrile and toluene. They explained that the rapid EN and subsequent ET is attributed to the folded conformation where the porphyrin and the C_{60} moieties locate with van der Waals contact, and with the pertubations of the absorption spectra, indicating the interaction between the two chromophores. The photoinduced EN and subsequent ET in their system is in sharp contrast to photophysical properties of **ZnP-P34-C$_{60}$**, **ZnP-M34-C$_{60}$**, and **ZnP-M23-C$_{60}$** where photoinduced ET is a main pathway in benzene and THF. The difference may be due to the magnitude of the electronic coupling between the two chromophores. **ZnP-O34-C$_{60}$** is similar to their model compound in that the two moieties are quite close to one another and show similar bathochromic shifts in the absorption spectra. If similar fast EN and subsequent fast ET ($>1 \times 10^{11}$ s^{-1}) occur in **ZnP-O34-C$_{60}$**, it is beyond the time resolution of our instrumentation. Such an experiment must await the instrumentation of femtosecond time-resolved fluorescence lifetime and transient absorption.

Linkage Dependence of Photoinduced CS and CR. Table 3 summarizes the CS and CR rates (k_{CS} and k_{CR}, respectively) in porphyrin-linked C_{60}. k_{CS1} ($= \tau_1^{-1}$ (at 600−650 nm) − τ_{ref1}^{-1}) and k_{CS2} ($= \tau_2^{-1}$ (at 720 nm or 750 nm) − τ_{ref2}^{-1}) were determined from the fitting of fluorescence decay due to the porphyrin and the C_{60}, respectively. k_{CR} was obtained by analyzing the absorbance due to the IP. It is difficult to determine the k_{CR} rates accurately in benzene because of the existence of two relaxation pathways from the IP state. The CS rates for all the porphyrin-linked fullerenes in C_6H_6 are comparable to those in THF. As the solvent dielectronic constant decreases, solvent reorganization energy (λ_s) and solvent stabilization of the IP state are reduced. Therefore, the CS in benzene may be in the top region of the Marcus curve, while that in THF be in the normal region owing to smaller reorganization energy (λ) in C_6H_6 compared with that in THF.[15]

As can be seen from Table 3, both CS and CR rates for **ZnP-M34-C$_{60}$** are much slower than those for the other porphyrin-linked C_{60}. Assuming that the Franck−Condon factor is similar thoughout the series and the ET takes place mainly through the σ- and π-bonds of the linkage, the trends in Table 3 can be accommodated by the superexchange mechanism,[24] since electronic coupling of the D and A via the *para* and *ortho* linkages should be stronger than that via the *meta* linkage. The superexchange coupling, V_{se}, between a D state (d) and an A state (a) via a linker state (l) is given by

$$V_{se} = (V_{dl}V_{la})/\Delta E_{dl}$$

where V_{dl} and V_{la} are the respective electronic coupling between (d) and (l), (l) and (a), and ΔE_{dl} is the energy difference between the states (d) and (l). The linker state (l) is a virtual state which simply increases the electronic coupling between the D and A states by mixing with them. In superexchange-mediated ET, the process could involve two concomitant transfers; one is an ET from the LUMO of the porphyrin D to the LUMO of the C_{60} A, mediated by the LUMO of the linker, and second is an ET in the opposite direction involving the HOMOs of the D, linker, and A.

Gust and Moore *et al.* explained triplet−triplet EN in porphyrin-carotenoid linked system by the superexchange mechanism.[25] Porphyrin and carotenoid are connected with similar linker via the aryl position, *para*, *meta*, and *ortho*, and the rates for the *meta* isomer are slower than those for the *para* and *ortho* isomers. Their results of Hückel molecular orbital calculations for the linkage show for both the HOMO and the LUMO the orbital density is greater at the *ortho* and *para* positions than it is at the *meta* position, which suggesting that the electronic coupling of the carotenoid and the porphyrin, as mediated by the superexchange interaction, will be greater at the *ortho* and *para* positions. As our porphyrin-C_{60} systems are quite similar to Gust and Moore model system, ET in our model compounds would also have to occur by the same mechanism as the case for the Gust's model compound. Such treatment has also reported by Osuka and Maruyama *et al.*[26] They have synthesized a series of carotenoid-bridged porphyrins where the rates of intramolecular singlet−singlet EN from the porphyrin to the carotenoid depend on the substitution pattern of the aromatic spacer. These spacer dependencies were interpretated by the similar superexchange mechanism involving via spacer.[27]

CS and CR rates for **ZnP-P23-C$_{60}$** is comparable to those for **ZnP-P34-C$_{60}$**. A possible explanation for this effect lies in the similar superexchange mechanism. Molecular orbital calculation with the PM3 method predicts HOMO and LUMO level in spacer unit of **ZnP-P34-C$_{60}$** (HOMO: −8.86 eV; LUMO: −0.376 eV) are parallel to those in spacer unit of **ZnP-P23-C$_{60}$** (HOMO: −9.01 eV; LUMO: −0.209 eV), suggesting

(23) (a) Wasielewski, M. R.; Minsek, D. W.; Niemczyk, M. P.; Svec, W. A.; Yang, N. C. *J. Am. Chem. Soc.* **1990**, *112*, 2823. (b) Lewis, F. D.; Burch, E. L. *J. Phys. Chem.* **1996**, *100*, 4055.

(24) (a) Kramers, H. A. *Physica* **1934**, *1*, 182. (b) Bixon, M.; Jortner, J.; Michel-Beyerle, M. E.; Ogrodnik, A. *Biochim. Biophys. Acta* **1989**, *977*, 273.

(25) Gust, D.; Moore, T. A.; Moore, A. L.; Devadoss, C.; Liddell, P. A.; Hermant, R.; Nieman, R. A.; Demanche, L. J.; DeGraziano, J. M.; Gouni, I. *J. Am. Chem. Soc.* **1992**, *114*, 3590.

(26) Osuka, A.; Yamada, H.; Maruyama, K.; Mataga, N.; Asahi, T.; Ohkouchi, M.; Okada, T.; Yamazaki, I.; Nishimura, Y. *J. Am. Chem. Soc.* **1993**, *115*, 9439.

(27) A number of examples of "through-bond" ET (which can be explained by the superchange mechanism) have been reported. (a) Closs, G. L.; Piotrowiak, P.; MacInnis, J. M.; Fleming, G. R. *J. Am. Chem. Soc.* **1988**, *110*, 2652. (b) Sigman, M. E.; Closs, G. L. *J. Phys. Chem.* **1991**, *95*, 5012. (c) Closs, G. L.; Miller, J. R. *Science* **1988**, *240*, 440. (d) Oevering, H.; Paddon-Row, M. N.; Heppener, M.; Oliver, A. M.; Cotsaris, E.; Verhoeven, J. W.; Hush, N. S. *J. Am. Chem. Soc.* **1987**, *109*, 3258. (e) Paddon-Row, M. N. *Acc. Chem. Res.* **1994**, *27*, 18.

ΔE_{dl} values are comparable in the both compounds. Hückel molecular orbital calculations also predict that electronic coupling of combination of the *para* and *meta* positions in **ZnP-P34-C_{60}** is similar to that of the *meta* and the *ortho* in **ZnP-P23-C_{60}**. Thus, the experimental results that the ET rate constants are comparable in **ZnP-P34-C_{60}** and **ZnP-P23-C_{60}** may be explained by the superexchange mechanism in the same fashion.

Comparison with Other Acceptors. Several groups have reported photophysical properties of porphyrin−porphyrin dyads.[28] In their molecules, zincporphyrin (ZnP) and freebase porphyrin (H_2P) were employed as a D and an A, respectively. By introducing substituents with electron-donating or electron-withdrawing ability into the porphyrin skeleton, driving force for intramolecular CS and CR can be varied. Singlet−singlet EN from the excited D to the A occurs, while both the porphyrin excited singlet states decay via photoinduced ET to the same IP ($ZnP^+-H_2P^-$) state. Although ratio of the both processes, EN and ET, depends upon the combination of D and A, they occur at the same time in many porphyrin−porphyrin dyads. This is sharp contrast with the results of our porphyrin-C_{60} systems; only photoinduced CS occurs regardless of solvents, separation distance, and the linkage between the two chromophores. Since porphyrins and fullerenes have both large π systems, the difference may be ascribed to those of global shapes (planar vs spherical) and of nature of the molecular orbitals. The characteristics are rather comparable to those of (porphyrin)-(small acceptor) systems, such as porphyrin-quinones and -pyromellitimides in which photoinduced CS from the excited singlet state of the porphyrin to the acceptor is a main pathway. However, CR is substantially slower than CS in our porphyrin-C_{60} systems, while CR is much faster than CS in many other porphyrin-quinone systems.[29] They may be explained by the smaller λ in C_{60} compared with that in quinone. Accordingly, our system with slow CR seems to offer new strategy for design of artificial photosythetic model with high yields of long-lived IP state.

Biological Applications. Many research groups have reported biological applications of fullerene and fullerene derivatives.[30] In terms of biological activity formation of singlet oxygen is crucial. Although we have not measured efficiency of singlet oxygen formation, efficient formation of $^3C_{60}$* in benzene was seen in all porphyrin-C_{60} compounds, indicating that singlet oxygen can be generated efficiently in our systems by selecting the linkage and solvents. In addition, the increase of the absorption cross section by both the chromophores also takes an advantage for the purpose. Therefore, porphyrin-C_{60} compounds will provide a new opportunity for design of photodynamic agents in cancer or viral therapy.

(28) (a) Gust, D.; Moore, T. A.; Moore, A. L.; Leggett, L.; Lin, S.; DeGraziano, J. M.; Hermant, R. M.; Nicodem, D.; Craig, P.; Seely, G. R.; Nieman, R. A. *J. Phys. Chem.* **1993**, *97*, 7926. (b) DeGraziano, J. M.; Liddell, P. A.; Leggett, L.; Moore, A. L.; Moore, T. A.; Gust, D. *J. Phys. Chem.* **1994**, *98*, 1758. (c) Osuka, A.; Marumo, S.; Maruyama, K.; Mataga, N.; Tanaka, Y.; Taniguchi, S.; Okada, T.; Yamazaki, I.; Nishimura, Y. *Bull. Chem. Soc. Jpn.* **1995**, *68*, 262.

(29) (a) Mataga, N.; Karen, A.; Okada, T.; Nishitani, S.; Sakata, Y.; Misumi, S. *J. Phys. Chem.* **1984**, *88*, 4650. (b) Frey, W.; Klann, R.; Laermer, F.; Elsaesser, T.; Baumann, E.; Futscher, M.; Staab, H. A. *Chem. Phys. Lett.* **1992**, *190*, 567. (c) Heitele, H.; Pöllinger, F.; Kremer, K.; Michel-Beyerle, M. E.; Futscher, M.; Voit, G.; Weiser, J.; Staab, H. A. *Chem. Phys. Lett.* **1992**, *188*, 270. (d) Hung, S. -C.; Lin, S.; Macpherson, A. N.; DeGraziano, J. M.; Kerrigan, P. K.; Liddell, P. A.; Moore, A. L.; Moore, T. A.; Gust, D. *J. Photochem. Photobiol. A: Chem.* **1994**, *77*, 207.

(30) Jensen, A. W.; Wilson, S. R.; Schuster, D. I. *Bioorg. Med. Chem.* **1996**, *4*, 767.

Conclusions

Summarizing the results of the present study, we have come to the following conclusions:

(1) It is shown that photoinduced CS and CR occur in porphyrin-C_{60} linked systems regardless of the linkage between the two chromophores.

(2) Depending on the solvent polarity and the separation distance, energy levels of the IP state in porphyrin-C_{60} linked systems vary. In THF the CS occurs from both the excited singlet state of the porphyrin and the C_{60} moieties. Although CS also occurs from the excited singlet state of the porphyrin to the C_{60} in benzene, CR process is quite different in that there are additional relaxation pathways from the IP state to locally excited singlet state of the C_{60} or energy equilibrium between the two states, in addition to the relaxation to the ground state.

(3) Both CS and CR rates for the *meta* isomer are much slower than those of the other porphyrin-linked C_{60}. Linkage dependence of the ET rates including the case of *meta* isomer can be explained by superexchange mechanism via spacer.

We could demonstrate experimentally that C_{60} can be used as an acceptor in artificial photosynthetic model systems. Our final goal in this research is to build up light-energy conversion system using new building block, C_{60}. Application of C_{60} seems to provide a new stage in synthesis and design of artificial photosynthetic models and photoactive materials. We are currently working on this line.

Experimental Section

Melting points were recorded on a Yanagimoto micro-melting apparatus and are not corrected. ^{1}H NMR, ^{13}C NMR, and 2D-COSEY spectra were measured on a JEOL EX-270. Mass spectra were obtained on a JEOL JMS-DX300. IR spectra were measured on a Perkin Elmer System 2000FT-IR as KBr disks. UV-visible spectra were obtained on a Hitachi 330 and Shimadzu UV3000. Fluorescence spectra were measured on Hitachi 850. Redox potentials were recorded on Bioanalytical Systems, Inc. CV-50W. Elemental analyses were performed on a Perkin-Elmer Model 240C elemental analyzer.

All solvents and chemicals were of reagent grade quality, purchased commercially, and used without further purification except as noted below. THF was distilled from benzophenone-Na. CH_2Cl_2 for use in electrochemical studies was distilled from CaH_2. Thin-layer chromatography (TLC) and flash column chromatography were performed on Art. 5554 DC-Alufolien Kiselgel 60 F_{254} (Merck), and Fujisilicia SW300, respectively.

Benzene was of spectrograde (Merck Uvasol) and was passed through a column of activated silica gel (Wako C-2000) for several times before spectroscopic use. THF (Merck Uvasol and Wako ∞Pure) was refluxed in the presence of molecular sieve (Wako 13X) and calcium hydride for 2 h and then distilled before spectroscopic use. The solution for optical measurements were deoxygenated by purging with nitrogen, and their concentrations were 10^{-6} M for the measurements of fluorescence lifetime and 10^{-4} M for time-resolved transient absorption spectroscopy.

Fluorescence decay curves were measured by means of a time-correlated single photon counting method using the second harmonic (400−403 nm) of Ti^{3+}:Al_2O_3 laser (Spectra-Physics, Tunami, FWHM 60−100 fs) pumped by Ar-ion laser (Spectra-Physics, Beamlock 2060).[31] SALS at the Osaka University Computation Center was used for the nonlinear least-squares analysis of the observed decay curves.

Picosecond transient absorption spectra were measured by means of a picosecond dye laser (FWHM 12 ps) pumped by the second harmonic of a repetitive mode-locked Nd^{3+}:YAG laser (Quantel, Picochrome YG-503 C/PTL-10).[32] The 590-nm output of the dye laser (Rhodamine 6G) was used for excitation.

(31) Nishikawa, S.; Asahi, T.; Okada, T.; Mataga, N.; Kakitani, T. *Chem. Phys. Lett.* **1991**, *185*, 237.

(32) Hirata, Y.; Okada, T.; Mataga, N.; Nomoto, T. *J. Phys. Chem.* **1992**, *96*, 6559.

Molecular orbitals were calculated by PM3, MOPAC Version 94.10 in CAChe, Version 3.7, CAChe Scientific, 1994.

Molecular mechanics calculations were performed using the CHARMm/QUANTA 4.0 program, Molecular Simulations Inc.

Acknowledgment. We thank Materials Analysis Center of ISIR for the measurement of FAB mass spectra. We are pleased to acknowledge the technical assistance of Hiromitsu Imamura, CTC Laboratory Systems Corporation for the molecular modeling. This work was supported by the Grant-in Aids (No. 07213220 and 07454166 to Y. S., No. 05NP0301 to T. O., and No. 08740495 to H. I.) from the Ministry of Education, Science, Sports and Culture, Japan. H. I. thanks Kansai Research Foundation for Technology Promotion and Foundation Advanced Technology Institute for financial support.

Supporting Information Available: The synthesis and characterization of porphyrin-linked fullerenes and related model compounds (20 pages). See any current masthead page for ordering and Internet access instructions.

JA9628415